Chapter 4

Digital Mammogram Enhancement

Michal Haindl and Václav Remeš

Additional information is available at the end of the chapter

http://dx.doi.org/10.5772/60988

1. Introduction

Three fully automatic methods for X-ray digital mammogram enhancement based on a fast analytical textural model are presented. These efficient single and double view enhancement methods are based on the underlying two-dimensional adaptive causal autoregressive texture model. The methods locally predict breast tissue texture from single or double view mammograms and enhance breast tissue abnormalities, such as the sign of a developing cancer, using the estimated model prediction statistics. The double-view mammogram enhancement is based on the cross-prediction of two mutually registered left and right breasts' mammograms or alternatively a temporal sequence of mammograms. The single-view mammogram enhancement is based on modeling prediction error in case of not the both breasts' mammograms being available.

Breast cancer is the most common type of cancer among middle-aged women in most developed countries [1, 2]. Almost one woman in ten grows a breast cancer in her life. According to the American Cancer Society [3] about 232 670 new cases of invasive breast cancer will be diagnosed in women and about 40 000 women will die from breast cancer in US alone. US mortality rate is 30% and European mortality rate is 45% [4].

To lower the mortality rate, women in the developed countries usually regularly attend a preventive mammography screening. However, around 25% of radiologically visible cancers are missed by the radiologists at screening [5]. This means that millions of cancer cases are missed and therefore even a slightest improvement in the detection methods could have a huge impact and save many lives.

The biggest problem with current Computer-Aided Diagnosis (CAD) systems is their large false negative rate and an even larger false positive rate. Most CAD systems (e.g., [1, 6]) point out 2-3 regions of interest (ROIs) per mammogram on average. Taking into account that there are about 8 malignant mammograms in 1000 [5], the radiologists consider the current CAD systems as misleading.

An alternative way is to automatically enhance mammograms to support radiologists with their visual mammogram evaluation. Several mammogram enhancement methods have been published [7–14]. Salvado and Roque [10] use wavelet analysis to detect microcalcifications, Dippel et al. [8] compare the merits of using either Laplacian pyramids or wavelet analysis for whole mammogram enhancement, Sakellaropoulos et al. [9] designed an adaptive wavelet based method for enhancing the contrast of the whole mammograms. Mencattini et al. [13] selectively enhance segmented mammograms regions using wavelet transformation.

An approach to diagnostic evaluation of screening mammograms based on local statistical Gaussian mixture textural models was proposed in [14]. The local evaluation tool has the form of a multivariate probability density of gray levels in a suitably chosen search window. First, the density function in the form of a Gaussian mixture is estimated from data obtained by scanning the mammogram with the search window. The estimated mixture is evaluated at each position and displays the corresponding log-likelihood value as a gray level at the window center. The resulting log-likelihood image closely correlates with the structural details of the original mammogram and emphasizes unusual places, but the method is very computationally demanding.

Radiologists regularly compare the bilateral mammogram pairs during mammogram screening in search for breast abnormalities. The mutual mammograms enhancement requires accurate registration of both breast X-ray images, which is difficult due to their elasticity. Marias et al. [15, 16] use thin-plate spline transformation [17] to align the breasts and then use wavelet based feature detection to find internal landmarks. Thin-plate spline based approach is also used by Wirth et al. in [18]. Hachama [19] deals only with the comparison of temporal mammograms based on a general method for registering images with the presence of abnormalities. However, it needs the prior abnormalities distribution knowledge. The registration and transformation are based on the Bayesian maximum a posteriori probability approach and minimization of the registration and deformation energy.

The novelty of our presented method is that whereas other alternative methods usually use simple pixel difference or trivial statistics like cross-correlation to compare the left and right images, we use the mammograms of one breast as a learning sample for the 2DCAR breast texture model [20, 21] and then try to analyze the other mammogram based on this acquired information. Using the 2DCAR model for bilateral comparison, we achieve a result which is robust to inaccurate registration, very fast, and which gives improved enhancement results compare to just a single-view analysis even using similar local texture modeling.

2. Public mammogram databases

There are not many publicly available mammogram databases [22–26], older databases like DDSM, MIAS are digitized from the X-ray films, while newer databases like INbreast are already digitaly acquired.

The Digital Database for Screening Mammography (DDSM) [24] http://marathon.csee.usf.edu/Mammography/Database.html is a database of digitized from original X-ray filmscreen in different resolutions and with associated ground truth and other information. This database was completed in 1999 and contains mammograms from four different sources using four different digitizers (DBA M2100 ImageClear, Howtek 960, Lumisys 200 Laser, Howtek MultiRad850) and 12 or 16 bits quantization. The database contains normal, benign,

and histologically proven cancerous mammograms in four different views (left and right cranio-caudal (CC) and medio-lateral oblique (MLO)). It contains breast imaging reporting and data system (BI-RADS) keywords and the American College of Radiology (ACR) tissue codes (Table 1).

ACR	Tissue density description	BI-RADS	Tumor description
-	unspecified	BI-RADS 0	unspecified
ACR-1	fat transparent system	BI-RADS 1	normal
ACR-2	fibroid glands system	BI-RADS 2	benign
ACR-3	heterogeneously dense	BI-RADS 3	probably benign
ACR-3/4	dense	BI-RADS 4	suspiciously abnormal
ACR-4	extremely dense	BI-RADS 5	malignant

Table 1. ACR and BI-RADS codes.

The Mammographic Image Analysis Society Digital Mammogram Database (miniMIAS) [22] is also digitized to 50 microns per pixel from the original X-ray filmscreen mammograms by the scanning microdensitometer SCANDIG3. MIAS mammographic images are available via the Pilot European Image Processing Archive (PEIPA) at the University of Essex http://peipa.essex.ac.uk/ipa/info/mias.html.

The LLNL/UCSF database ftp://gdo-biomed.ucllnl.org/pub/mammo-db/ [23] contains 198 digitized films from 50 patients with 4 views per patient (but only 2 views from one mastectomy case).

The INbreast database [26] is a mammographic database, with images acquired at a Breast Centre, located in a University Hospital (Hospital de São João, Breast Centre, Porto, Portugal). INbreast has a total of 115 cases (410 images) of which 90 cases are from women with both breasts (4 images per case) and 25 cases are from mastectomy patients (2 images per case). Several types of lesions (masses, calcifications, asymmetries, and distortions) are included. Accurate contours made by specialists are also provided in the XML format.

The recent BancoWeb LAPIMO Database http://lapimo.sel.eesc.usp.br/bancoweb/ [27] was acquired in two hospitals using Senographe 500t and Senographe 600t mammographs and digitized by using two laser scanners Lumiscan 50 and Lumiscan 75.

The overview of major features of the public mammographic databases are listed in the following Table 2.

3. Mammogram enhancement methods

The mammogram enhancement methods can be roughly categorized into frequency based and spatial based methods. The frequency based methods [7, 9, 28, 29] use mostly some wavelet multiscale decomposition with modified wavelet coefficients to enhance mammogram contrast. The spatial methods [14, 30] use some nonlinear or adaptive linear filters.

We have implemented four representative mammogram enhancement methods from several published alternatives [7–10, 10–14] to compare with our novel adaptive probabilistic mammogram enhancement method.

	DDSM ([24])	INbreast ([26])	miniMIAS ([22])	LLNL ([23])	LAPIMO ([27])
n_{mam}	10480	410	322	198	1473
n_{views}	4	4	2	4	4
n_{gl}	16/12	14	8	12	12
x *resolution*	$1411-5641$	$2560-3328$	1024		
y *resolution*	$3256-7111$	$3328-4084$	1024		
normal	695	70	204	38	294
↓*benign*	141	116		128	994
benign	870	44	66		
malignant	914	180	52	32	112
density	*ACR*	*ACR*	*own scale*	*no*	*no*
BI-RADS	*yes*	*yes*	*no*	*no*	*yes*

Table 2. Public Mammogram Databases: where (n_{mam}) is the number of mammograms, (n_{views}) number of views, (n_{gl}) number of gray levels in bits, and ↓is benign without callback.

3.1. Histogram equalization

The well known gray scale image enhancement technique is histogram equalization [31], which is based on the idea of forcing the enhanced image histogram to be uniform. This is a popular technique for contrast enhancement because because of its simplicity and effectivity. However, it may overenhance the noises and sharp regions in the original images.

3.2. Matting-based enhancement

The enhancement method based on the idea of image matting was published in [32]. It works based on the idea that mammographic images (Y) are a superposition of some background adipose tissue (B) and the interesting part, which would be the mammary glands and other breast structures (G).

$$Y = Gc + B(1-c) \tag{1}$$

The enhancement method then selectively subtracts the background tissues from the superposition, thus creating the enhanced image.

To enable this, the authors had to estimate the background (B) and the opacity alpha value for each pixel by which it is blended with the rest of the image (c). In this method the background is set as a constant value for the whole image represented by the 85% percentile of grey values of the breast part of the image.

3.3. Nonlinear unsharp masking

A nonlinear unsharp masking (NLUM) combined with nonlinear filtering for mammogram enhancement was introduced in [33]. The method embeds different types of filters into the nonlinear filtering operator within the 3×3 window which fuses the enhanced and original mammogram data. The unsharp masking emphasizes high-frequencies of the signal either by subtracting a low-pass filtered signal from its original or adding a scaled high-frequency factor to the measured original. NLUM eight parameters are optimized using the proposed second-derivative-like measure of enhancement (SDME) [33].

3.4. Direct contrast enhancement

An enhancement method based on wavelet transformation was described in [29]. The method performs a multi-level 2D wavelet transfomation and at each level the 3 highpass components are divided by the lowpass-lowpass component, getting a directional contrast estimate, which is further multiplied by a constant contrast enhancement factor λ. Starting at the deepest level of the transform, the inverse transform is performed one scale at a time. For each scale level, before the inverse transform step, the 3 modified components are multiplied by the newly computed lowpass component. This way the authors achieve a contrast enhancement without the introduction of too much of additional noise.

4. Probabilistic mammogram enhancement

These our methods use Markovian texture models for the analysis of local texture characteristics and enhancing breast tissue abnormalities such as microcalcifications and masses which could be the sign of a developing cancer. We make the presumption that left and right breasts are architecturally symmetrical. This presumption is indeed reasonable, since radiologists frequently compare double-view mammograms to find asymmetrical parts, which could indicate a developing cancer. The texture based symmetry detection neither needs to assume the pixel-wise correspondence of the both breast images, nor their ideal sub-pixel registration inside the breast area.

The double-view methods consist of three major steps: registration, model parameters adaptive estimation, and the cross-prediction based analysis.

4.1. Mammogram registration

The registration process is described for mammographic MLO views, but it can be easily adapted also for CC views. Since we compare the images based on textural features rather than pixel-wise, we do not require as precise registration as other methods, and can use a simple registration based on the affine transformation.

Three reference points are needed for the affine transformation (Figure 1). We chose the nipple and one point above and one below that are closest to the pectoral muscle.

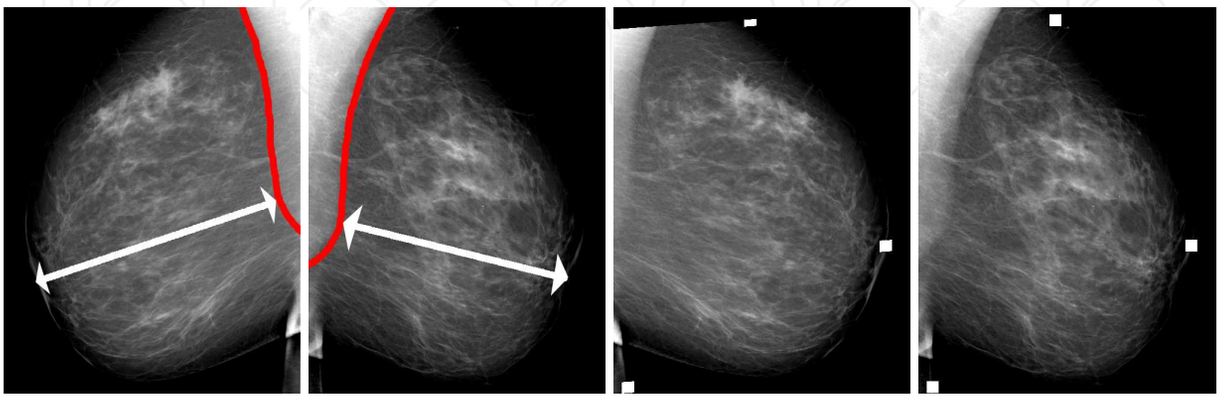

Figure 1. Registered mammograms with visible reference points.

The nipple is located using the heuristic method described in [34]. It works on the idea of the nipple being a point on the skin-line of the breast which is the most distant from the line of the pectoral muscle. After the candidates for the nipple reference points have been found in both the mammograms, the position of the reference point can still slightly differ in both images. Therefore, we adjust their position by searching the neighborhood on the skin line of the breast for the most correlated window.

The remaining reference point candidates have to be further adjusted as well. Since the bilateral mammograms usually do not cover the same area of the breast, some anatomical parts of the breast can be seen only in one of the images and therefore the reference points wouldn't match. To make up for this problem, we measure the distance of the points to the nipple, weighted by the nipples distance to the pectoral muscle. The weighting compensates for the differences of positioning of the breast in the mammogram which could result in one image displaying the breast bigger than the other. We then adjust the corresponding reference points, so that they are on the skin line with the most similar weighted distance to the nipple possible.

Having found the reference points, the affine transformation is performed. Figure 1 in the leftmost images shows the images of right and left breast with marked line of the pectoral muscle (colored in red) and the distance from the pectoral muscle to the nipple. The rightmost images show the registered breasts with the reference points painted as white squares with the right breast (shown on the left side) transformed to match the left breast.

4.2. Adaptive textural model

The X-ray mammographic tissue is locally modeled by its dedicated independent Gaussian noise-driven autoregressive random field two-dimensional texture model (2DCAR), which is a rare exception among Markovian random field model family that can be completely analytically solved [35, 36]. Apart from that, this descriptive model has good modeling performance, all statistics can be evaluated recursively, and the model is very fast to evaluate.

The 2DCAR random field is a Markovian family of random variables with a joint probability density on the set of all possible realizations Y of the $M \times N$ lattice I, subject to the following condition:

$$p(Y \mid \gamma, \sigma^{-2}) = (2\pi\sigma^2)^{-\frac{(MN-1)}{2}} \exp\left\{\frac{-1}{2} tr\left\{\sigma^{-2}\begin{pmatrix}-\alpha\\ \gamma^T\end{pmatrix}^T \tilde{V}_{MN-1}\begin{pmatrix}-\alpha\\ \gamma^T\end{pmatrix}\right\}\right\}, \quad (2)$$

where α is a unit vector, $tr()$ is a trace of the corresponding matrix, and the following notation is used

$$\tilde{V}_{r-1} = \sum_{k=1}^{r-1}\begin{pmatrix} Y_k Y_k^T & Y_k X_k^T \\ X_k Y_k^T & X_k X_k^T \end{pmatrix} = \begin{pmatrix} \tilde{V}_{y(r-1)} & \tilde{V}_{xy(r-1)}^T \\ \tilde{V}_{xy(r-1)} & \tilde{V}_{x(r-1)} \end{pmatrix}.$$

Here, $r = [r_1, r_2, \phi]$ is spatial multiindex denoting history of movements on the rectangular lattice I, where r_1, r_2 are row and column indices, and the direction of the model development is $\phi \in \{0°, 45°, 90°, 135°, 180°, 225°, 270°, 315°\}$. The 2DCAR model can be expressed as a stationary causal uncorrelated noise-driven 2D autoregressive process:

$$Y_r = \gamma_\phi X_r + e_r \ , \tag{3}$$

where $\gamma_\phi = [a_1, \ldots, a_\eta]$ is the parameter vector, $\eta = cardinality(I_r^c)$, I_r^c denotes a causal (or alternatively unilateral) contextual neighborhood (i.e., all support pixels were previously visited and thus they are known). Elements in I_r^c do not need to be topological neighbours of each other, i.e., if s is a neighbour of r then $\exists t, t \in I$ located between r and s at a distance $\delta(r,t) < \delta(r,s)$ such as $t \notin I_r^c$. This type of a neighbourhood system is also called a functional neighbourhood system and its application is illustrated in Figure 2. Its optimal configuration can be found analytically using the Bayesian statistics see [36] for details. Furthermore, e_r denotes white Gaussian noise with zero mean and a constant but unknown variance σ^2, and X_r is a support vector of Y_{r-s} where $s \in I_r^c$. The method uses a locally adaptive version of this 2DCAR model [36], where its recursive statistics are modified by an exponential forgetting factor, i.e., a constant smaller than 1 which is used to weight the older data.

4.2.1. Parameter estimation

Parameter estimation of the 2DCAR model using either the maximum likelihood, the least square or Bayesian methods can be found analytically. The Bayesian parameter estimates of the 2DCAR model using the normal-gamma parameter prior are:

$$\hat{\gamma}_{r-1}^T = V_{x(r-1)}^{-1} V_{xy(r-1)} \ , \tag{4}$$

$$\hat{\sigma}_{r-1}^2 = \frac{\lambda_{(r-1)}}{\beta(r)} \ , \tag{5}$$

where

$$\begin{aligned} \lambda_{(r-1)} &= V_{y(r-1)} - V_{xy(r-1)}^T V_{x(r-1)}^{-1} V_{xy(r-1)} \ , \\ V_{(r-1)} &= \tilde{V}_{(r-1)} + V_{(0)} \ , \\ \beta(r) &= \beta(0) + r - 1 \ , \end{aligned}$$

and $\beta(0)$ is an initialization constant and submatrices in $V_{(0)}$ are from the parameter prior. The parameter estimates (4),(5) can also be evaluated recursively [36] using the proces history ($Y^{(r-1)}$). The posterior probability density [36] of the model is:

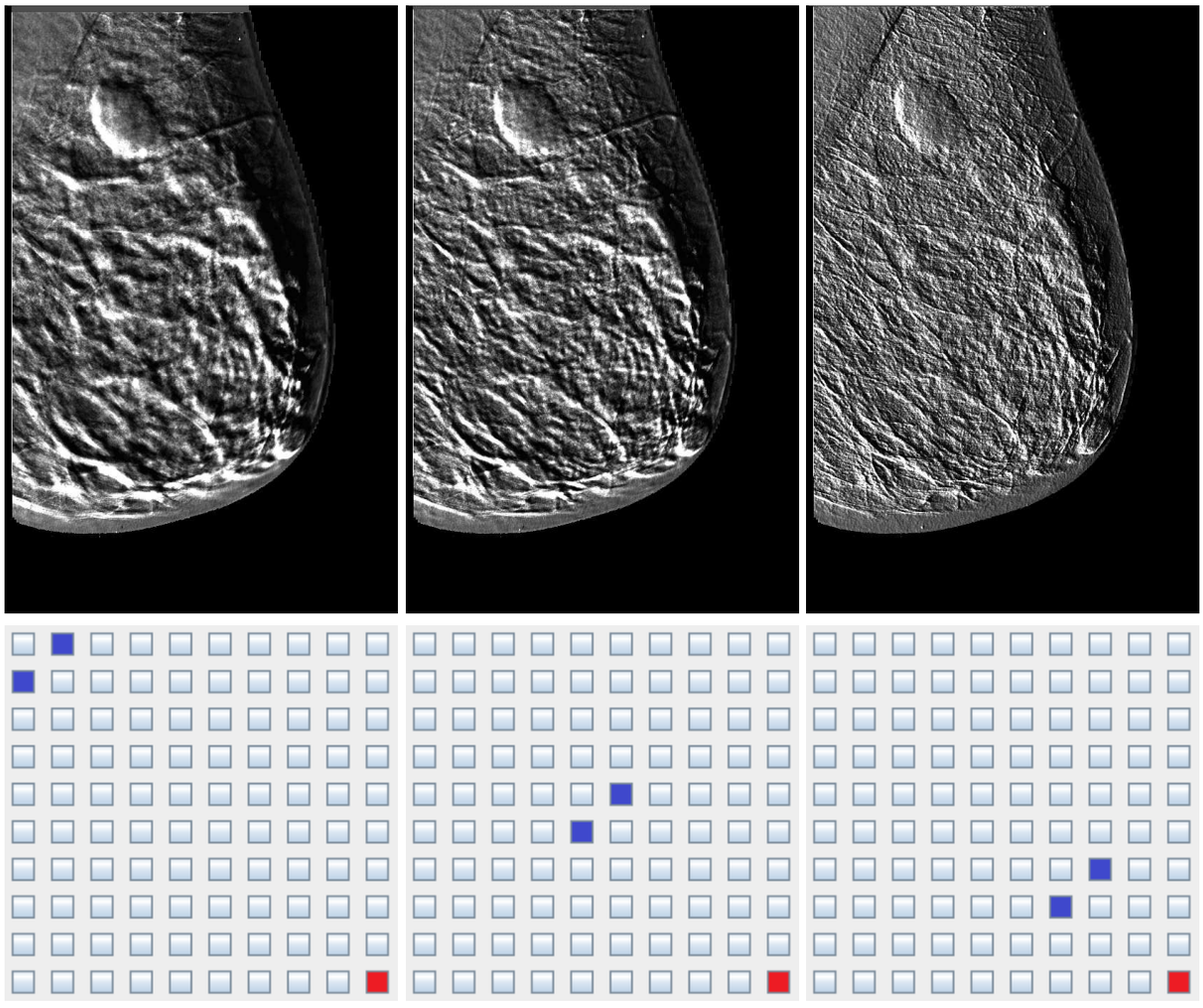

Figure 2. Single-view MLO mammogram enhancement using different functional neighbourhoods consecutively rightwards - 9, 5, and 3 pixel neighbourhood distance from the enhanced pixel (blue pixels - bottom row).

$$p(Y_r \mid Y^{(r-1)}, \hat{\gamma}_{r-1}) = \frac{\Gamma(\frac{\beta(r)-\eta+3}{2})}{\Gamma(\frac{\beta(r)-\eta+2}{2})\ \pi^{\frac{1}{2}}\ (1+X_r^T V_{x(r-1)}^{-1} X_r)^{\frac{1}{2}}\ |\lambda_{(r-1)}|^{\frac{1}{2}}} \left(1+\frac{(Y_r-\hat{\gamma}_{r-1}X_r)^T \lambda_{(r-1)}^{-1}(Y_r-\hat{\gamma}_{r-1}X_r)}{1+X_r^T V_{x(r-1)}^{-1} X_r}\right)^{-\frac{\beta(r)-\eta+3}{2}} \tag{6}$$

And the conditional mean value predictor of the one-step-ahead predictive posterior density (6) for the normal-gamma parameter prior is

$$E\left\{Y_r \mid Y^{(r-1)}\right\} = \hat{\gamma}_{r-1} X_r \ . \tag{7}$$

http://dx.doi.org/10.5772/60988

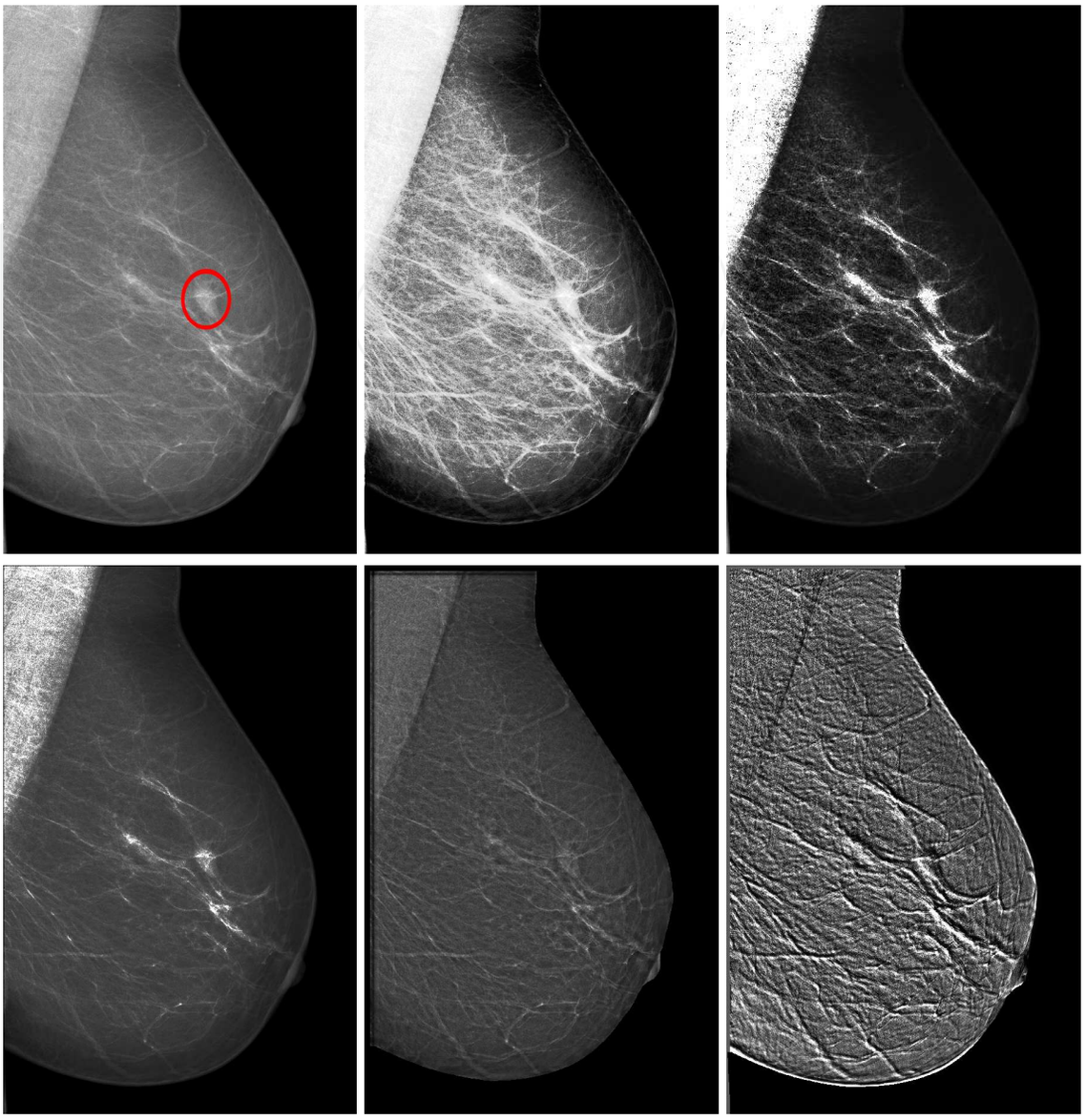

Figure 3. INbreast MLO mammogram enhancement comparison rightwards: the original mammogram, histogram equalization, [32], [33], [29], and the presented enhancement methods, respectively.

4.2.2. Prediction

The conditional mean value of the one-step-ahead predictive posterior density for the normal-gamma parameter prior is

$$E\left\{Y_r \mid Y^{(r-1)}\right\} = \hat{\gamma}_{r-1} X_r \ . \tag{8}$$

The predictor (8) is used only for single-view mammogram enhancement. For double-view mammograms where there are available both left and right breasts mammograms the method uses the cross-prediction (10),(11).

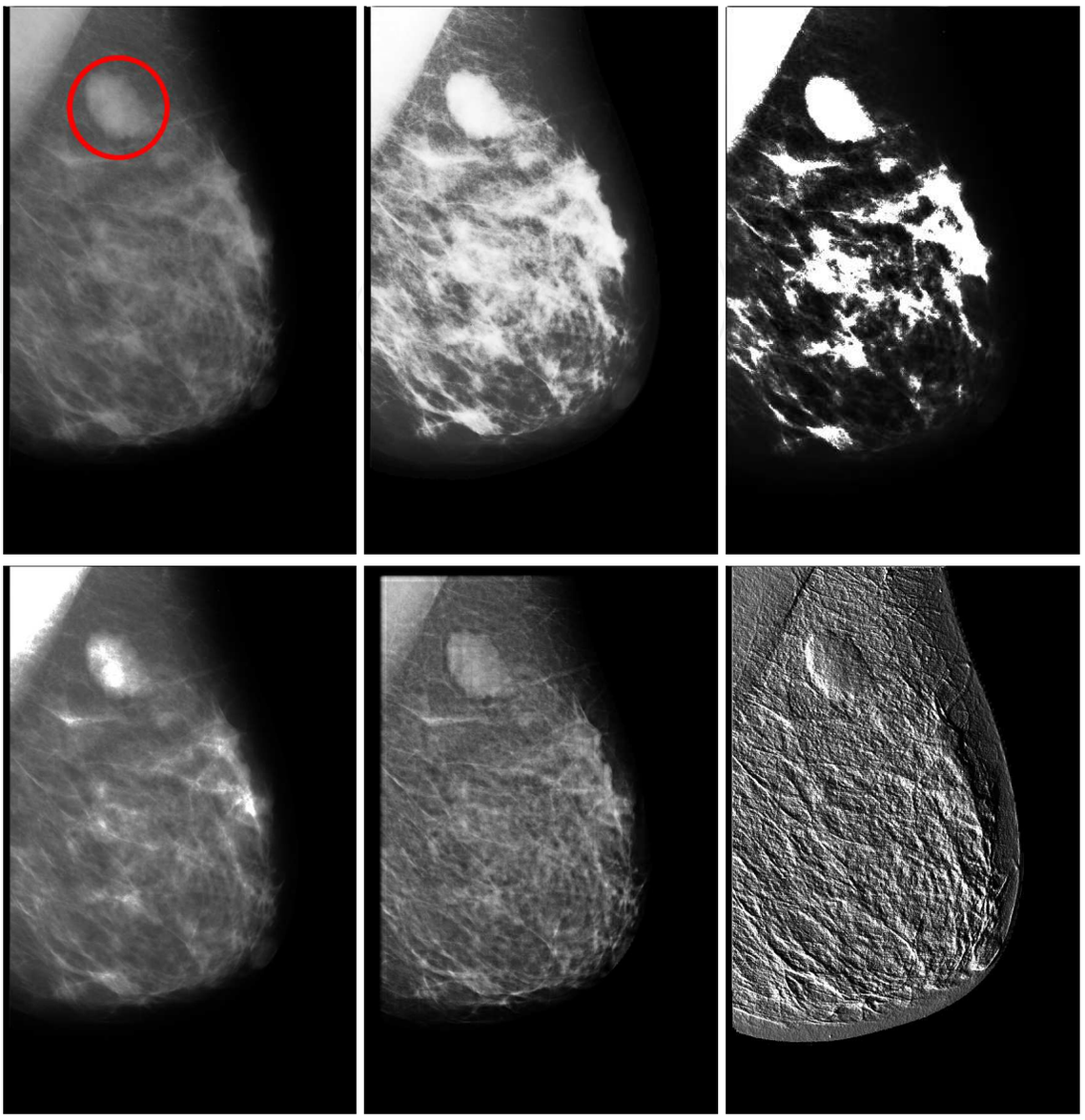

Figure 4. MIAS MLO mammogram enhancement comparison rightwards: the original mammogram, histogram equalization, [32], [33], [29], and the presented enhancement methods, respectively.

4.3. Enhancement methods

Let us denote two mutually registered (e.g., left and right breasts') mammograms Y and $\tilde{Y}$, the local 2DCAR model parameters estimates (4), (5) computed on the mammogram image Y $\hat{\gamma}_{r-1}^T, \hat{\sigma}_{r-1}^2$. The same parameter estimates (4), (5) computed on the other mammogram $\tilde{Y}$ are denoted $\tilde{\gamma}_{r-1}^T, \tilde{\sigma}_{r-1}^2$, and the corresponding support vector is $\tilde{X}_r$. The directional models are computed in the following angles $\phi \in \Phi = \{0°, 45°, 90°, 135°, 180°, 225°, 270°, 315°\}$.

4.3.1. Single-view enhancement

The single-view enhacement method is computed from up to eight directional models, i.e.,

http://dx.doi.org/10.5772/60988

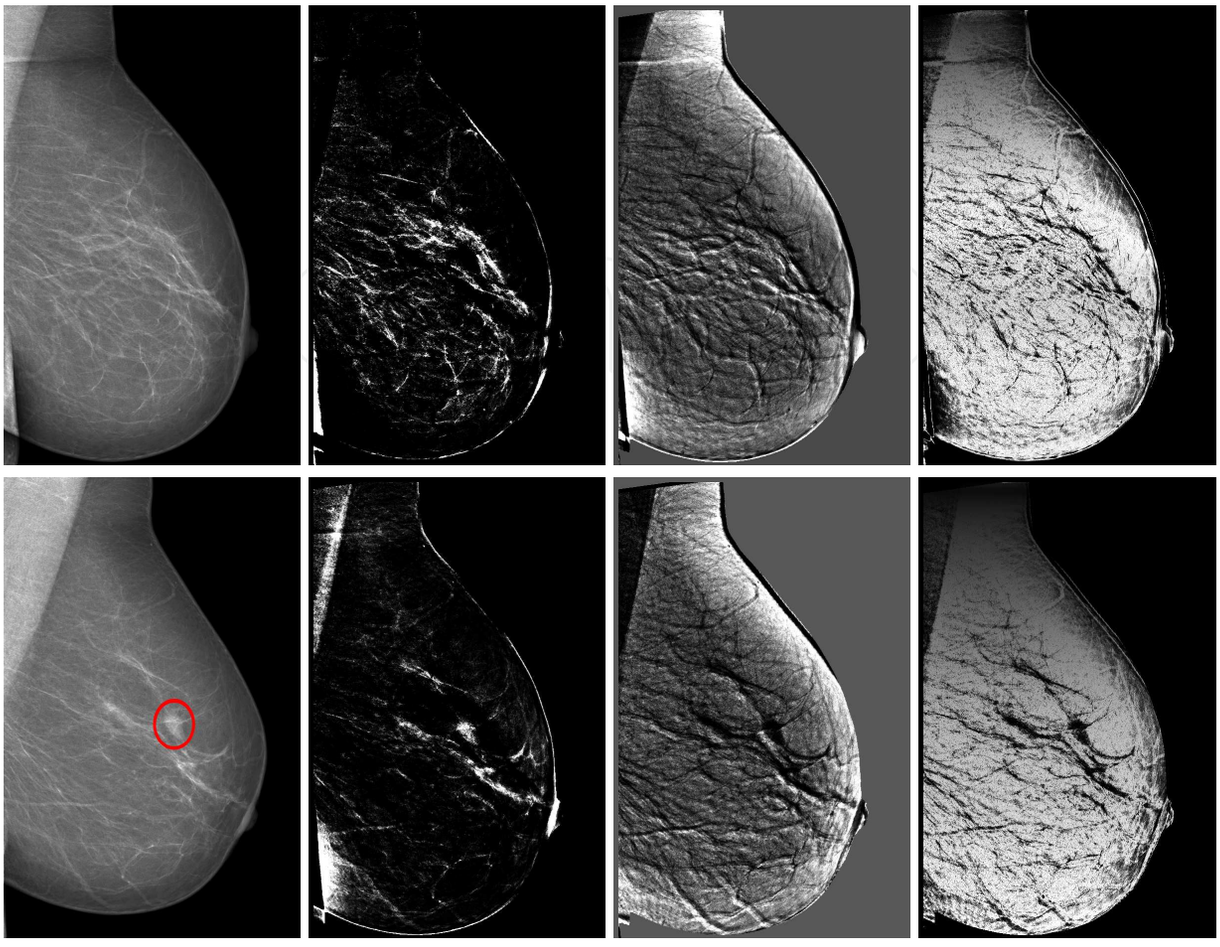

Figure 5. INbreast multiple-view MLO mammogram enhancement consecutively rightwards - ground truth, pixel difference between registered LMLO and RMLO, cross-predicted gradient, and cross-prediction probability density. The upper row contains LMLO, bottom row RMLO.

$$Y_r^{enh} = \sum_{\forall \phi \in \bar{\Phi}} \left(Y_{r+1} - \hat{\gamma}_{r-1} X_r \right) \ , \tag{9}$$

where $\bar{\Phi} \subseteq \Phi$. All the enhanced values are normalized into the $0-255$ range.

4.3.2. Double-view enhancement

The double-view enhancement is based on statistics computed on one breast image and applied to the complementary one. The cross-prediction between images $Y, \tilde{Y}$ is computed as follows:

$$E\left\{ \tilde{Y}_r \mid Y^{(r-1)} \right\} = \hat{\gamma}_{r-1} \tilde{X}_r \tag{10}$$

and the opposite direction cross-prediction is analogously

$$E\left\{Y_r \mid \tilde{Y}^{(r-1)}\right\} = \tilde{\gamma}_{r-1} X_r \ . \tag{11}$$

The enhanced mammograms are then the corresponding cross-prediction statistics images. The corresponding cross-prediction probability densities are $p(\tilde{Y}_r \mid \tilde{Y}^{(r-1)}, \hat{\gamma}_{r-1})$ and $p(Y_r \mid Y^{(r-1)}, \tilde{\gamma}_{r-1})$.

The proposed double-view enhancement methods are

$$Y_r^{com_1} = \sum_{\forall \phi \in \bar{\Phi}} \left(\tilde{Y}_{r+1} - \hat{\gamma}_{r-1} X_r\right) \ , \tag{12}$$

$$Y_r^{com_2} = \sum_{\forall \phi \in \bar{\Phi}} p(\tilde{Y}_r \mid \tilde{Y}^{(r-1)}, \hat{\gamma}_{r-1}) \ . \tag{13}$$

5. Experimental results

The comparative experimental results (Figures 3, 4) were tested on the miniMIAS database [22] and on the state-of-the-art public digital mammogram INbreast database [26]. Comparing the alternative methods (Section 3) with our proposed adaptive enhancement, it is clearly visible that whereas these methods enhance prevailingly contrast, our method enhances textural abnormalities in the breast tissue which is more useful for the radiologists.

Our adaptive enhancement methods were also successfully tested on the Digital Database for Screening Mammography (DDSM) from the University of South Florida [24]. These results are reported elsewhere.

The spatial textural model allows seamless and natural generalization into multiple-view mammogram enhancement (be it bilateral, as presented in Figures 5, 6, or temporal). Double-view medio-lateral oblique digital mammograms' enhancements from the INbreast database (Figure 5) and the miniMIAS database (Figure 6) show the cross-prediction based enhancement performance. Comparing the cross-prediction enhancements on Figures 5, 6 respectively with the same breast single-view enhancements on Figures 3, 4, the benefits of the cross-prediction are clearly visible.

Both our double-view enhancement methods are compared with the registered image pixel difference which is standardly used for comparison ([15, 18, 19])

$$\Delta Y_r = max\{Y_r^R - Y_r^L, 0\} \ . \tag{14}$$

This standard double-view enhancement method (Figures 5, 6 - second columns) is inferior compared to the both proposed double-view enhancement methods ((12), (13)) which simultaneously exhibit more contrast and increased details' visibility.

Finally, all three proposed enhancement methods are very fast - they can be computed on the presented mammograms with a standard PC in a matter of several seconds.

http://dx.doi.org/10.5772/60988

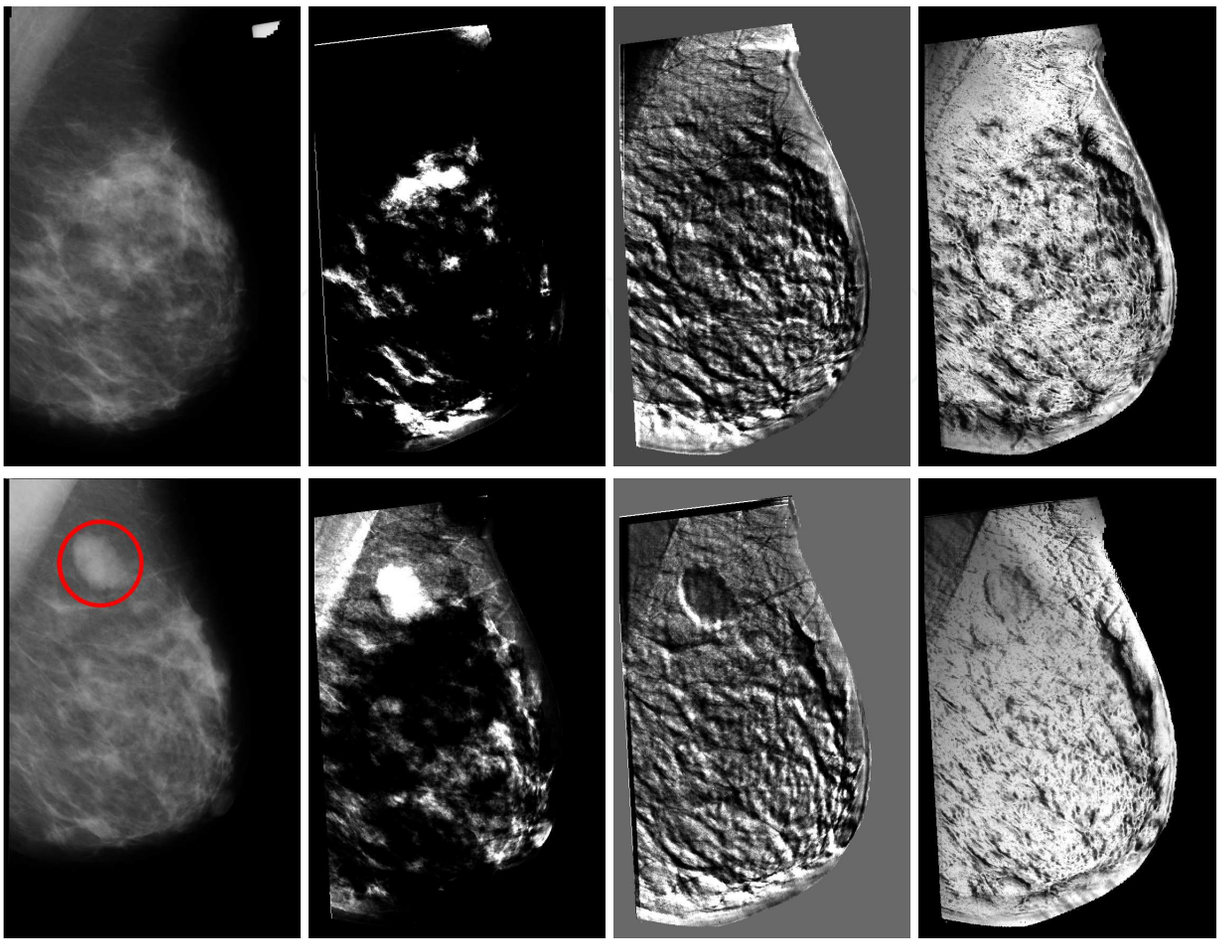

Figure 6. Multiple-view medio-lateral mammogram (INbreast) enhancement consecutively rightwards - ground truth, pixel difference between registered LMLO and RMLO, cross-predicted gradient, and cross-prediction probability density. The upper row contains LMLO, bottom row RMLO.

6. Conclusions

We proposed three novel fast methods for completely automatic mammogram enhancement which highlight regions of interest, detected as textural abnormalities. Cancerous areas typically manifest themselves in X-ray mammography as such textural defects which is advantageous for our methods in comparison with most alternative mammogram enhancement methods that primarily enhance only the image contrast. Thus the enhanced mammograms can help radiologists to decrease their false negative evaluation rate.

These methods are based on the underlying two-dimensional adaptive CAR texture model. Although the algorithms use random field type model, the model is very fast due to the efficient recursive model predictor estimation and therefore is much faster than the usual alternative Markov chain Monte Carlo estimation approach. The enhancement can be either single or double view depending on the available data. The single-view methods allow significant mammogram enhancement without the need of paired mammogram registration. The double-view methods benefit from mutual textural information in the registered bilateral breast pairs. Contrary to the simple pixel difference values or cross-correlations, the textural feature comparison brings increased robustness to registration inaccuracies

inevitably encountered due to the elasticity of the breast. The double-view methods could alternatively be used for the enhancement of a temporal sequence of mammograms.

Acknowledgements

This research was supported by the Czech Science Foundation project GAČR 14-10911S.

Author details

Michal Haindl and Václav Remeš

The Institute of Information Theory and Automation of the Czech Academy of Sciences, Prague, Czech Republic

References

[1] Tweed, T.; Miguet, S. Automatic Detection of Regions of Interest in Mammographies Based on a Combined Analysis of Texture and Histogram. In *Pattern Recognition, 2002. Proceedings. 16th International Conference on*, Vol. 2; IEEE Computer Society: Los Alamitos, CA, USA, 2002.

[2] Qi, H.; Diakides, N. A. Thermal Infrared Imaging in Early Breast Cancer Detection - A Survey of Recent Research. In *Proceedings of the 25th Annual International Conference of the IEEE Engineering in Medicine and Biology Society*, Vol. 2; 2003.

[3] ACS, "Breast cancer facts & figures 2011 -? 2012", Technical Report, American cancer society, 2012.

[4] Kopans, D. B. *Radiology* 2010, *256*, 15–20.

[5] Taylor, P. and Champness, J. and Given-Wilson, R. and Johnston, K. and Potts, H., *Health Technology Assessment* 2005, *9*,.

[6] Haindl, M.; Mikeš, S.; Scarpa, G. Unsupervised Detection of Mammogram Regions of Interest. In *Knowledge-Based Intelligent Information and Engineering Systems*, Vol. 4694; Apolloni, B.; Howlett, R. J.; Jain, L., Eds.; Springer: 2007.

[7] Chang, C.-M.; Laine, A. *IEEE Transactions on Information Technology in Biomedicine* 1999, *3*, 32–46.

[8] Dippel, S.; Stahl, M.; Wiemker, R.; Blaffert, T. *Medical Imaging, IEEE Transactions on* 2002, *21*, 343–353.

[9] Sakellaropoulos, P.; Costaridou, L.; Panayiotakis, G. *Physics in medicine and biology* 2003, *48*, 787.

[10] Salvado, J.; Roque, B. Detection of calcifications in digital mammograms using wavelet analysis and contrast enhancement. In *Intelligent Signal Processing, 2005 IEEE International Workshop on*; 2005.

[11] Yan, Z.; Zhang, Y.; Liu, B.; Zheng, J.; Lu, L.; Xie, Y.; Liang, Z.; Li, J. Extracting hidden visual information from mammography images using conjugate image enhancement software. In *Information Acquisition, 2005 IEEE International Conference on*; IEEE: 2005.

[12] Thangavel, K.; Karnan, M.; Sivakumar, R.; Mohideen, A. *Graphics, Vision and Image Processing* 2007, 55–60.

[13] Mencattini, A.; Salmeri, M.; Lojacono, R.; Frigerio, M.; Caselli, F. *Instrumentation and Measurement, IEEE Transactions on* 2008, *57,* 1422–1430.

[14] Grim, J.; Somol, P.; Haindl, M.; Daneš, J. *IEEE Transactions on Image Processing* 2009, *18,* 765 - 773.

[15] Marias, K.; Behrenbruch, C. P.; Brady, M.; Parbhoo, S.; Seifalian, A. Multi-scale landmark selection for improved registration of temporal mammograms. In *International Workshop on Database Machines*; 2000.

[16] Marias, K. and Behrenbruch, C. and Parbhoo, S. and Seifalian, A. and Brady, M., *Medical Imaging, IEEE Transactions on* 2005, *24,* 782–790.

[17] Harder, R L and Desmarais, R N, *Journal of Aircraft* 1972, *9,* 189–191.

[18] Wirth, M. A.; Narhan, J.; Gray, D. A model for nonrigid mammogram registration using mutual information. In *In International Workshop on Digital Mammography*; 2002.

[19] Hachama, M. and Richard, F. and Desolneux, A., A mammogram registration technique dealing with outliers. In *Biomedical Imaging: Nano to Macro, 2006. 3rd IEEE International Symposium on*; 2006.

[20] Haindl, M.; Havlíček, V. A multiscale colour texture model. In *Pattern Recognition, 2002. Proceedings. 16th International Conference on*, Vol. 1; 2002.

[21] Haindl, M.; Šimberová, S. *Theory & Applications of Image Analysis* 1992, 306–315.

[22] Suckling, J. *et al.* The mammographic image analysis society digital mammogram database. In *2nd International Workshop on Digital Mammography*; International Congress Series Excerta Medica: 1994.

[23] LLNL, "Lawrence Livermore National Library / UCSF Digital Mammogram Database", Technical Report, Center for Health Care Technologies Livermore, Lawrence Livermore National Library, Livermore, CA, USA, 1995.

[24] Heath, M.; Bowyer, K.; Kopans, D.; Moore, R.; Kegelmeyer, P. The Digital Database for Screening Mammography. In *Proc. of the 5th Int. Workshop on Digital Mammography*; Medical Physics Publishing: 2000.

[25] Oliveira, J. E.; Gueld, M. O.; Araújo, A. d. A.; Ott, B.; Deserno, T. M. Toward a standard reference database for computer-aided mammography. In *Medical Imaging*; 2008.

[26] Moreira, I. C.; Amaral, I.; Domingues, I.; Cardoso, A.; Cardoso, M. J.; Cardoso, J. S. *Academic radiology* 2012, *19,* 236–248.

[27] Matheus, B. R. N.; Schiabel, H. *Journal of digital imaging* 2011, *24,* 500–506.

[28] Mencattini, A.; Caselli, F.; Salmeri, M.; Lojacono, R. Wavelet based adaptive algorithm for mammographic images enhancement and denoising. In *Image Processing, 2005. ICIP 2005. IEEE International Conference on*, Vol. 1; 2005.

[29] Tang, J.; Liu, X.; Sun, Q. *Selected Topics in Signal Processing, IEEE Journal of* 2009, *3,* 74–80.

[30] Dhawan, A. P.; Buelloni, G.; Gordon, R. *Medical Imaging, IEEE Transactions on* 1986, *5,* 8–15.

[31] Pratt, W. K. *Digital image processing: PIKS inside;* John Wiley & Sons, Inc: 2007.

[32] Wang, H.; Li, J.-B.; Wu, L.; Gao, H. *Clinical imaging* 2013, *37,* 273–282.

[33] Panetta, K.; Zhou, Y.; Agaian, S.; Jia, H. *Information Technology in Biomedicine, IEEE Transactions on* 2011, *15,* 918–928.

[34] Georgsson, F.; Ols?n, C. The accuracy of geometric approximation of the mamilla in mammograms. In *CARS'03*; 2003.

[35] Haindl, M. *CWI Quarterly* 1991, *4,* 305-331.

[36] Haindl, M. Visual Data Recognition and Modeling Based on Local Markovian Models. In *Mathematical Methods for Signal and Image Analysis and Representation*, Vol. 41; Florack, L.; Duits, R.; Jongbloed, G.; Lieshout, M.-C.; Davies, L., Eds.; Springer London: 2012 10.1007/978-1-4471-2353-8_14.